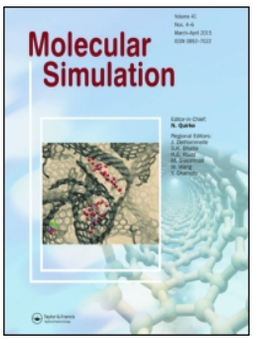

Molecular Simulation

ISSN: 0892-7022 (Print) 1029-0435 (Online) Journal homepage: http://www.tandfonline.com/loi/gmos20

Electronic structure of boron-doped finite graphene sheets: unrestricted DFT and complete active space calculations

Ana E. Torres, Reyes Flores, Lioudmila Fomina & Serguei Fomine

To cite this article: Ana E. Torres, Reyes Flores, Lioudmila Fomina & Serguei Fomine (2016) Electronic structure of boron-doped finite graphene sheets: unrestricted DFT and complete active space calculations, Molecular Simulation, 42:18, 1512-1518, DOI: 10.1080/08927022.2016.1214955

To link to this article: http://dx.doi.org/10.1080/08927022.2016.1214955

MOLECULAR SIMULATION, 2016
VOL. 42, NO. 18, 1512–1518
http://dx.doi.org/10.1080/08927022.2016.1214955

Taylor & Francis
Taylor & Francis Group

Electronic structure of boron-doped finite graphene sheets: unrestricted DFT and complete active space calculations

Ana E. Torres, Reyes Flores, Lioudmila Fomina and Serguei Fomine

Instituto de Investigaciones en Materiales, Universidad Nacional Autónoma de México, Coyoacán, Mexico

ABSTRACT

B3LYP and complete active space methods were applied to study graphene nanoribbons (GNRs) doped with boron atoms. The restricted B3LYP solutions were found to be unstable in all but two cases, and the complete active space calculations prove the multiconfigurational character of the ground state contributing with two most important configurations. The exception is the structure **c4** where the system has single reference ground state in spite of the instability of the restricted wavefunction.

The distance between dopant atoms, their mutual position and their location within the nanoribbon impact the relative stability of doped nanoribbons. B doping does not modify the ionisation potentials of doped GNRs. However, it notably increases the electron affinity of the core-doped nanoribbons. The doping also has a notable impact on the reorganisation energy of the nanoribbons. The reorganisation energy of B-doped GNRs is higher than the corresponding reorganisation energy of pristine and nitrogen-doped GNRs.

ARTICLE HISTORY
Received 5 May 2016
Accepted 13 July 2016

KEYWORDS
Graphene; DFT; restricted active space; multiconfigurational; boron; doping

1. Introduction

Recently, graphene has been widely explored due to its unique physical and electronic properties, since it could be one of the most promising materials to use in electronic devices.[1,2] It is the study on graphene and related bidimensional systems that attracted attention to the area of graphene nanoribbons and nanoflakes. The graphene nanoribbons (GNRs) represent graphene fragments of nanometric size. Unlike graphene, GNRs have a band gap, which allows for multiple applications in the field electronics.[3] It has been suggested that the structures fabricated from GNRs would become important elements for nanoelectronics. Nowadays, these structures have been prepared and they were found to have higher electron mobilities compared to graphene.[4–6]

The geometric parameters and chemical composition of GNRs were found to play an important role in determining their properties. Therefore, the doping allows one to tune the graphene electronic properties and their energy gap, similar to that in the silicon-based technology.[7] One of the most common methods is the substitutional doping, when heteroatoms such as boron or nitrogen replace some of the carbon atoms of the sp^2 lattice of graphene. As it has been recently discovered, GNRs possess multiconfigurational character of the ground state, showing strong polyradicalic character in some cases.[8] This fact put in doubt the applicability of single reference methods for the study of GNRs and related systems.

A very similar situation holds for the nitrogen-doped GNR.[9] N-doped GNRs also show a multireference ground state (singlet or triplet) independently on the type of nitrogen atom (pyridinic or graphitic). The separation of dopant atoms affects the nature of the ground state. GNRs where graphitic dopants are well separated have closed-shell singlet ground state. It should be noted that the use of single reference methods strongly underestimates ionisation potentials (IP) of pristine or N-doped GNRs as compared to complete active space (CAS) calculations. [9]

Boron has one electron less than carbon and two electron less than nitrogen, and it is thought to produce *p*-type defects.[10] However, like nitrogen, a different position of the dopant in GNR will produce a defect with different electronic nature (Figure 1).

As seen, the doping in the core produces defects with no shared π-electrons at all, while the doping in the edge generates a doping site with one shared π-electron.

There are numerous publications both experimental and theoretical describing the synthesis and electronic properties of B-doped GNRs. Experimental data reveal that boron doping decreases the energies of graphene bands.[11] Calculations at DFT level suggested that nanostructures containing both boron and nitrogen dopant atoms are half metals.[12] Nevertheless, the half-metallicity in extended systems could be an artefact, since it has been shown that the exact treatment of the electron correlation,[13] is able to cancel it. The vast majority of the theoretical calculations on B-doped GNRs has been done within the framework of periodic boundary conditions or closed-shell DFT; however, it is very important to use more rigorous theoretical treatment for the study of B-doped GNRs to obtain deeper insight into their electronic structure. The goal of this paper was to study B-doped GNRs using CAS and broken symmetry (BS) dispersion-corrected DFT methods and compare the results with the existing experimental and also theoretical data.

CONTACT Serguei Fomine fomine@unam.mx

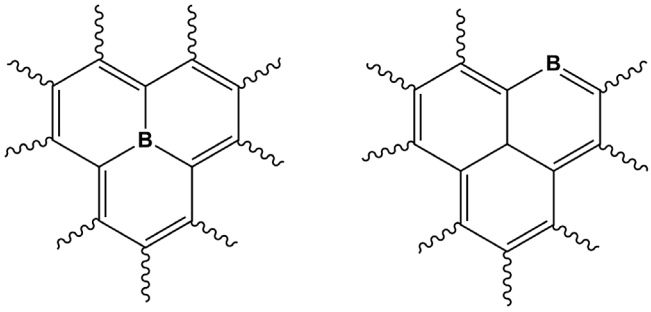

Figure 1. Different types of boron defects in graphene.

2. Computational details

The geometry of the pristine and boron-doped (GNR)-type structures was optimised at D3-B3LYP [14] level of theory as implemented in Turbomole 7.0 [15] with the Dunning's correlation consistent cc-pVDZ basis set.[16] The geometry optimisations were performed with spin restricted methods for the singlet electronic states, while in the case of the triplet states, the unrestricted DFT method was employed.

The SCF triplet stability test was carried for the closed-shell singlet solution. Thus, as an alternative to the restricted DFT approach, in the case of triplet instability, the molecular geometry was reoptimised within the framework of the broken symmetry unrestricted method (BS-UB3LYP).

In order to explore the multiconfigurational character of the ground state of the analysed molecules, a single-point energy CAS calculation was run at B3LYP-optimised geometries of the corresponding electronic multiplicity. The Pople's 6-31G (d) 5d basis set was assigned to all atoms.[17] The chosen active space consisted of 10 electrons in 10 orbitals which included relevant orbital interactions for these kinds of systems as π-orbitals of the conjugated systems and the p-orbital of boron. These multireference calculations were carried out with Gaussian 09 rev. D.01 program package.[18]

To study the boron-doping effect, it has been selected a rectangular graphene nanoribbon type structure of size **m** × **n** (where **m** and **n** are the number of fused benzene rings which define the width and length of the structure, respectively). This structure corresponds to a (**R4, 6**) rectangular graphene nanoribbon. According to a previous research, the ground state of analogue systems has shown an important multiconfigurational character,[9] with only moderate polyradicalic character since the most important contributions to the CAS wavefunction correspond to closed-shell singlet configurations.

With the aim to explore the boron-doping effect, 2 atoms of boron were incorporated into the pristine structure. This corresponds to ~1.6% atom. It must be mentioned that similar structures have already been synthesised experimentally.[4]

The doping sites for boron were chosen to cover maximum number of non-equivalent positions and to match the position of nitrogen-doped systems from our previous work to allow the direct comparison of nitrogen- and boron-doped systems. Moreover, the effect of the separation between doping sites has been additionally studied, which was found to be very important for N-doped GNRs (Figure 2).[9]

The hole (λ_+) and the electron reorganisation energies (λ_-) of the GNRs were calculated using the following equations:

$$\lambda_+ = \left(E_n^+ - E_n\right) + \left(E_+^n - E_+\right)$$

$$\lambda_- = \left(E_n^- - E_n\right) + \left(E_-^n - E_-\right)$$

where E_n, E_+ and E_- are the energies of the neutral, cationic and anionic species in their lowest energy geometries. E_n^+ and E_+^n are the energies of the neutral and cationic species with the geometries of the cationic and neutral species, respectively.

3. Results and discussion

The relative energies of different electronic states calculated for boron-doped graphene nanoribbons are shown in Tables 1 and 2. The stability test performed for restricted B3LYP solutions detected triplet instability for all but **c5** and **c7** neutral species; therefore, 'polyradicalic' states (PRS) with the multiplicity 1 were also calculated using BS UB3LYP. UDFT produces unphysical spin densities since unrestricted Hamiltonian does not commute with S^2 operator. However, due to the nature of BS unrestricted wavefunction, it describes better multireference systems than restricted one does. In agreement with the variational principle, the unrestricted wavefunction is a better approximation to the exact solution since it corresponds to the lower energy state.

As seen from Table 1, the energetic stability of the edge-doped B-GNRs generally increases with the separation between boron atoms at DFT level, for both restricted and unrestricted solutions. The difference between the most stable (e5) and the less stable system (**e1**) is close to 10 kcal/mol. The ground state is singlet for all edge-doped systems at DFT level, although triplet and singlet states are almost degenerated at DFT level. CAS calculations indicate that **e5** is the most stable isomer out of all edge-doped systems, in agreement with DFT; however, CAS predicts triplet ground state for **e2** and **e4**, and also indicating that **e4** is the less stable isomer.

There is no clear dependence of the system stability on the separation between dopant atoms for the core-doped systems (Table 2). According to DFT, the most stable core-doped isomer is **c1** and the less stable is **c6**. However, the separation between doping atoms affects the nature of the ground state of B-GNRs. As seen, systems **c7** and **c5**, with the most separated boron atoms have stable closed-shell wavefunctions, producing closed-shell singlet ground state. This phenomenon has already been observed for nitrogen-doped GNR.[9]

According to DFT, the ground state for all core-doped B-GNRs is singlet except for **c2**. However, singlet and triplet states are almost degenerated at DFT level. The only exceptions are the systems **c5** and **c7**, with closed-shell singlet states. The results of DFT and CAS calculations agree on that **c1** is the most stable isomer. Both methods DFT and CAS predict triplet ground state for **c2** isomer. Therefore, DFT and CAS show a reasonable agreement between the relative energies of B-GNRs and the nature of the ground state. It is noteworthy that the calculated CAS single-point energies depend notably on the choice of the method used for the geometry optimisation in the case of

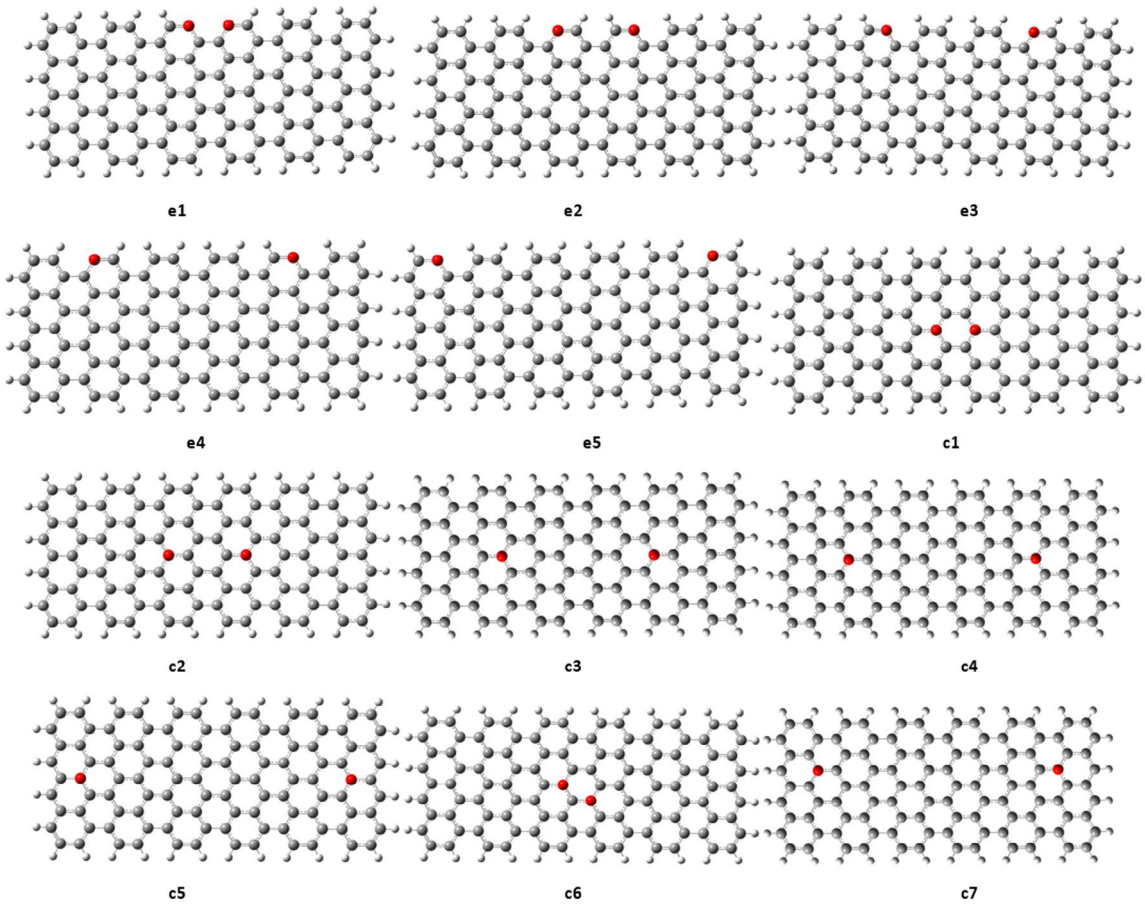

Figure 2. (Colour online) B-GNRs studied structures; edge doped (**e1**-**e5**) and core doped (**c1**-**c5**, **a**, and **i**).

Table 1. Relative electronic energies calculated for B-GNRs doped in the edges (kcal mol^{-1}). RB3LYP/cc-pVDZ optimised closed-shell singlet (S0), UB3LYP/cc-pVDZ broken symmetry polyradicalic (PRS) and triplet (T) states. CAS(10,10)/6–31G(d) single-point relative energies estimated for the corresponding DFT-optimised geometries

	B3LYP			CAS(10,10)		
GNR	S0	PRS	T	S0	PRS	T
e1	26.75	9.05	9.10	11.42	21.79	21.79
e2	23.99	6.35	6.40	9.38	2.29	2.20
e3	21.88	4.36	4.41	17.90	9.45	14.82
e4	22.77	5.09	5.14	19.02	15.23	14.82
e5	16.66	0.00[a]	0.01	0.00[b]	28.07	28.03

[a]Reference state for DFT energy.
[b]Reference state for CAS energy.

Table 2. Relative electronic energies calculated for B-GNRs doped in the core (kcal mol^{-1}). RB3LYP/cc-pVDZ optimised closed-shell singlet (S0), UB3LYP/cc-pVDZ broken symmetry polyradicalic (PRS) and triplet (T) states. CAS(10,10)/6–31G(d) single-point relative energies estimated for the corresponding DFT-optimised geometries

	B3LYP			CAS		
Structure	S0	PRS	T	S0	PRS	T
c1	17.68	0.00[a]	0.00	9.14	0.00[b]	7.51
c2	33.37	24.23	17.06	69.25	69.98	59.92
c3	24.08	7.39	7.43	27.86	28.12	33.24
c4	15.70	14.62	15.79	59.56	50.31	67.45
c5	9.68	–	12.99	21.93	–	38.12
c6	38.66	21.40	21.81	69.43	42.72	42.35
c7	11.95	–	19.02	41.91	–	42.20

[a]Reference state for DFT energy.
[b]Reference state for CAS energy.

Table 3. Squared CI expansion coefficients for dominant configurations in GNRs at CAS(10,10)/6–31G(d) level of theory for closed-shell singlet (S0), polyradicalic state (PRS) and triplet using B3LYP/cc-pVDZ optimised geometries.

	S0		PRS		Triplet
GNR	2222200000	2222020000	2222200000	2222020000	2222aa0000
pristine	0.420	0.420	0.420	0.420	0.884
e1	0.242	0.382[a]	0.449	0.449	0.897
e2	0.422	0.420	0.423	0.423	0.845
e3	0.446	0.443[a]	0.437	0.435	0.909
e4	0.437	0.438	0.403	0.404	0.909
e5	0.430	0.470	0.472	0.471	0.943
c1	0.437	0.436	0.328	0.328	0.871
c2	0.192	0.194[a]	0.869	0.017[a]	0.897
c3	0.431	0.432[a]	0.00	0.013[a]	0.900
c4	0.924	0.010	0.906	0.000	0.936
c5	0.842	0.000	–[a]	–[a]	0.900
c6	0.452	0.434[a]	0.424	0.426	0.860
c7	0.823	–	–[a]	–[a]	0.845

[a]RB3LYP solution is stable.

singlets, restricted or BS unrestricted method. This difference can achieve 26 kcal/mol (isomer **c6**, Table 2). In the most, but not all the cases, the use of BS unrestricted optimised geometry leads to the lower energies at CAS single-point energy calculation for the singlet state and, therefore, it is thought that BS unrestricted method generally delivers better molecular geometry.

The multiconfigurational character of the ground states can be reviewed examining the CI expansion coefficients of the CAS wavefunction. They are shown in Table 3

Table 3 depictures squared CI expansion coefficients for the most important configurations in B-GNRs at CAS(10,10)/6-31G(d) level of theory for the closed-shell singlet (S0), the polyradicalic state (PRS) and the triplet (T) using B3LYP/cc-pVDZ optimised geometries. As seen from Table 3, the pristine and most of the doped GNRs singlet states have notable multiconfigurational character. On the other hand, the triplet states are all single reference states due to the smaller amount of static correlation of triplets. Singlet states of **c4**, **c5** and **c7** are the single reference ones as seen from the large squared CI expansion coefficients for principal configurations. **C5** and **c7**, systems with larger separation between boron atoms, have a stable closed-shell wavefunction and as a consequence single reference singlet ground state. The same situation has also been observed for N-doped GNRs [9] where systems with large separation between doping centres have single reference singlet ground state. **C4**, however, has an unstable closed-shell singlet wavefunction with $<S^2>$ expectation value of 0.91 for unrestricted BS singlet B3LYP solution, suggesting that triplet instability is not always an indication of the multiconfigurational character of the electronic state (Table 4). However,$<S^2>$ expectation value for **c4** is still the lowest one out of all other doped systems possessing a multiconfigurational singlet state.

Triplet states show only moderate spin contamination in all cases and especially for **c5** and **c7**. Table 5 shows calculated (IP's) and electron affinities (EA's) of B-GNRs.

As seen, when PRS state is taken as reference state, IPs are higher and EAs are lower compared to S0 taken as a reference. This is due to lower energy of PRS state compared to S0 one. Unfortunately, no experimental data are available for IP's of GNRs. The only possible comparison can be done with graphene work function (4.3 eV).[19] Actually, the graphene work function is very similar to the calculated IP for pristine GNR estimated

Table 4. $<S^2>$ expectation values for polyradicalic (PRS), triplet state (T), cationic (C) and anionic (A) species at the B3LYP/cc-pVDZ level.

Structure	PRS	T	C	A
Pristine		2.11	0.80	0.78
e1	1.12	2.11	0.81	0.79
e2	1.12	2.11	0.81	0.79
e3	1.12	2.11	0.81	0.79
e4	1.12	2.11	0.81	0.79
e5	1.10	2.10	0.79	1.10
c1	1.11	2.12	0.81	1.86
c2	1.79	2.52	1.13	1.83
c3	1.11	2.11	0.80	1.85
c4	0.91	2.42	0.77	0.81
c5	–[a]	2.05	0.76	0.80
c6	1.51	2.34	1.29	1.86
c7	–[a]	2.07	0.78	0.92

[a]RB3LYP solution is stable.

with restricted S0 state as the reference state (4.43 eV). However, it is very well known that IPs of conjugation systems decrease systematically with its size.

Therefore, the employment of a restricted S0 electronic state as the reference state for the ionisation potential underestimates the IP for pristine GNR. It is been shown earlier [8] that BS unrestricted B3LYP generates IP's values near these obtained with CAS technique that have errors for conjugated hydrocarbons of solely few tenths of eV above experimental values.[20] Considering this, it looks that UB3LYP offers reasonable estimation of IP in spite of large spin contamination in the neutral state. This has been well proven for N-doped GNRs.[9]

The edge doping generates chemically equivalent doping sites for B and N dopants, everyone sharing one π-electron with the GNR π-electron system. The additional lone pair of nitrogen is orthogonal to the GNR plane (pyridine nitrogen), thus not interacting with π-electron cloud. The core doping produces chemically different sites for nitrogen and boron. Boron has no π-electrons at all to share, providing only empty p-orbital, while nitrogen shares 2p electrons with the π-electron system of GNR. This difference leads to the p-type doping for the edge-doped N-GNRs and n-type doping for core-doped N-GNRs.[9] As seen from Table 5, for the systems **c6**, **c1** and **c7** where both B-GNR and N-GNR IP's and EA's data are available, the IPs of N-GNRs are notably lower than those of B-GNRs reflecting the effect of the lone electron pair which increases the electron repulsion. The

Table 5. Adiabatic ionisation potentials (IP) and electron affinities (EA) obtained at B3LYP/ cc-pVDZ theory level (e*V*) using closed-shell singlet (S0) and polyradicalic (PRS) states. The difference of natural charges for boron atoms between cationic and neutral (Δ^+) and anionic and neutral (Δ^-) states at UB3LYP/cc-pVDZ level of theory.

Structure	IP (S0)	IP (PRS)	EA (S0)	EA (PRS)	Δ^+	Δ^-
Pristine	4.43	5.19	−2.90	−2.13	–	–
e1	4.39	5.16	−2.89	−2.12	0.024	−0.021
e2	4.41	5.17	−2.90	−2.14	0.020	−0.017
e3	4.34	5.10	−2.84	−2.08	0.042	−0.035
e4	4.42	5.19	−2.93	−2.16	0.018	−0.012
e5	4.10	4.82	−2.62	−1.90	0.117	−0.083
c1	4.46 (3.96)[a]	5.23 (4.74)[a]	−3.31 (2.84)[a]	−2.54 (2.06)[a]	0.018	−0.194
c2	4.52	4.91	−3.02	−3.02	0.010	−0.050
c3	4.44	5.16	−3.65	−2.93	0.003	−0.110
c4	4.99	5.03	−2.90	−2.86	−0.041	−0.047
c5	4.91	–	−2.83	–	0.086	−0.021
c6	4.43 (3.54)[a]	5.18 (4.27)[a]	−3.68 (2.82)[a]	−2.94 (2.08)[a]	0.043	−0.038
c7	5.20 (4.55)[a]	–	−2.81 (2.10)[a]	–	0.003	0.018

[a]Corresponding N-doped GNR [9].

same mechanism is responsible for lower EAs of the core-doped N-GNRs compared to B-GNRs.

Unlike N-GNR, in the case of B-GNR, there are no clear differences in IPs between the edge and the core-doped systems; moreover, for the systems where boron atoms are not very far from each other, IPs are similar to these of pristine GNR (Table 5).

While the core-doped systems have their IPs close to the edge doped and pristine GNR, they show notably higher EAs due to the presence of a vacant *p*-orbital on B atoms. Thus, for **c2,** EA is almost 1 e*V* higher compared to pristine GNR. The presence of empty *p*-orbitals on B atoms in the core-doped B-GNRs also notably increase the EAs of B-GNRs compared to N-GNRs.[9]

The difference between the core- and the edge-doped B-GNR is also reflected in the variation of the natural charges for boron atoms between neutral and charged species at DFT level (Table 5). As seen from Table 5, B defects generally have a significantly higher fraction of delocalised extra electron of the anion radicals in core-doped systems compared to the edge-doped ones. These data indicate that core doping with boron atoms results in *p*-doped materials in agreement with [10].

A vital task within the understanding of the conductivity of the doped GNRs is to characterise the structural factors essential in the charge transfer rates. It has been shown that the solid-state hole mobility in arylamines [21] and conjugated oligomers [22] is determined by the reorganisation energy. When isolated molecule shows low internal reorganisation energy, the solid-state charge carrier mobility (when combined with strong electronic coupling) normally is high. This is important point for the fabrication of the highly efficient electronic devices. It is known that the majority of organic semiconductors have their internal reorganisation energies larger than 0.1 eV.[23] It is noteworthy that, although a few *p*-type organic semiconductors have been reported with internal reorganisation energies (λ_+) of less than 0.1 eV, only limited number of π-type acceptors shows electron reorganisation energies (λ_-) of less than 0.1 eV.[24] Fullerene C60 is one of them with reorganisation energy of (0.060 eV).

The reorganisation energy depends on the size of the conjugated system, decreasing with its extension. Thus, triphenylene has reorganisation energy of 0.18 eV, coronene 0.13 eV and hexa-peri-hexabenzocoronene 0.1 eV.[25–27]

The charge transport mechanism in GNRs also depends on its size. Thus, in the case of large GNR (40 nm wide), the ballistic mechanism is operational.[5] However, for smaller systems, all experimental data point to hopping mechanism.[28] Table 6 summarises calculated λ_+ and λ_- for pristine and doped GNRs.

Although we were unable to find any experimental data on reorganisation energy of pristine or doped GNRs, we believe that the reorganisation energy of pristine GNR is less than 0.1 e*V*. The best DFT method to calculate the reorganisation energies of organic conjugated systems was found to be B3LYP. [29,30]

It has been demonstrated that restricted B3LYP delivers unphysical values for the reorganisation energies of GNRs. UB3LYP method, on the other hand, gives physically meaningful results.[8] Only for systems **c5** and **c7,** the data of RB3LYP were used since these systems have a closed-shell ground state. As seen from Table 6, all doped systems have notably higher reorganisation energies compared to pristine GNR. A similar situation has been observed for N-doped GNRs, although, in general, the reorganisation energies for both electrons and holes are lower for N-doped systems compared to B-doped ones. The difference between N-GNRs and B-GNRs reorganisation energies is related to different C-B and C-N bond strengths. C-N bond energy is higher compared to C-B one,[31] thus providing more rigidity to N-GNRs compared to B-GNRs that could lead to lower reorganisation energies for N-GNRs. There is no clear difference between the electron and the hole reorganisation

Table 6. Reorganisation energies for electrons (λ_-) and holes (λ_+) (eV) estimated using the UB3LYP method.

Structure	λ_-	λ_+
Pristine	0.020	0.021
e1	0.0350	0.0325
e2	0.0366	0.0339
e3	0.0324	0.0383
e4	0.0381	0.0360
e5	0.0286	0.0371
a	0.0830	0.1172
c1	0.0582	0.0356
c2	–[a]	–[a]
c3	0.0884	0.0449
c4	0.0448	0.0274
c5	0.0347[b]	0.0819[b]
c6	0.0830	0.1172
c7	0.0403[b]	0.0670[b]

[a]SCF not converged.
[b]RB3LYP reference state was used.

energies for B-GNRs; however, they clearly depend on the location of the doping sites. Thus, the edge-doped systems have lower reorganisation energies than the core ones. This is related to the fact that in the edge-doped systems, B atoms have only two neighbouring carbons atoms unlike core doping where there are three of them. Therefore, edge defects affect less the electronic structure and the reorganisation energies of GNRs compared to the core ones.

Similar to N-GNRs, the largest reorganisation energies for the core-doped B-GNRs are those with *meta* mutual position of dopant atoms (structure **c6**). We observed no clear dependence of the reorganisation energies on the separation distance between doping centres.

4. Conclusions

The relative stability of B-GNRs is connected with the mutual position of the dopant atoms and also the position of N atoms within the nanoribbon. Both methods DFT and CAS agree on the lowest energy isomers which are **e5** and **c1** for the edge- and core-doped systems, respectively. Doping influences the multireference character of B-GNR. Thus, for the models **c4**, **c5** and **c7** where boron atoms are well separated from each other, the ground state is single reference even though **c4** shows instability of the closed-shell state.

In spite of the significant multiconfigurational character detected for the majority of the singlet ground states, B-GNRs only exhibited two dominant closed-shell singlet configurations. All triplets are single reference ground states since static correlation is less important for triplets compared to singlets.

Core-doped systems have their IPs close to the edge-doped and pristine GNR; however, they show notably higher EAs due to the presence of vacant *p*-orbital on B atoms. The presence of the empty *p*-orbitals on B atoms in the core-doped B-GNRs also notably increases EAs of B-GNRs compared to N-GNRs confirming *p*-type doping for the core-doped systems.

The doping changes the reorganisation energy of B-GNRs, being always higher than the reorganisation energies for pristine- and N-doped GNRs. Moreover, the core-doped GNRs have higher reorganisation energies compared to the edge-doped ones.

Acknowledgments

We acknowledge to thank the General Direction of Computing and Information Technologies and Communication of the National Autonomous University of Mexico (DGTIC-UNAM) for the support to use the supercomputer facilities. A.E. Torres gratefully acknowledges Consejo Nacional de Ciencia y Tecnología (CONACyT) for a graduate scholarship (245467) and R. Flores states his gratefulness to CONACyT for the postdoctoral fellowship (173315).

Funding

This work was supported by Program to Support Research and Technological Innovation Projects (PAPIIT) [grant number IN100215/27].

References

[1] Geim AK, Novoselov KS. The rise of graphene. Nat. Mater. 2007;6:183–191.
[2] Castro Neto AH, Guinea F, Peres NMR, et al. The electronic properties of graphene. Rev. Mod. Phys. 2009;81:109–162.
[3] Vo TH, Shekhirev M., Kunkel DA, et al. Large-scale solution synthesis of narrow graphene nanoribbons. Nat. Commun. 2014;5:3189. doi: http://dx.doi.org/10.1038/ncomms4189
[4] Cai J, Ruffieux P, Jaafar R, et al. Atomically precise bottom-up fabrication of graphene nanoribbons. Nature. 2010;466:470–473.
[5] Baringhaus J, Ruan M, Edler F, et al. Exceptional ballistic transport in epitaxial graphene nanoribbons. Nature. 2014;506:349–354.
[6] Chernozatonskii LA, Sorokin PB, Artukh AA. Novel graphene-based nanostructures: Physicochemical properties and applications. Russ. Chem. Rev. 2014;83:251–279.
[7] Usachov D, Vilkov O, Grüneis A, et al. Nitrogen-doped graphene: Efficient growth, structure, and electronic properties. Nano Lett. 2011;11:5401–5407.
[8] Torres AE, Guadarrama P, Fomine S. Multiconfigurational character of the ground states of polycyclic aromatic hydrocarbons. A systematic study. J. Mol. Model. 2014;20:2208 1–9.
[9] Torres AE, Fomine S. Electronic structure of graphene nanoribbons doped with nitrogen atoms: a theoretical insight. Phys. Chem. Chem. Phys. 2015;17:10608–10614.
[10] Huang B. Electronic properties of boron and nitrogen doped graphene nanoribbons and its application for graphene electronics. Phys. Lett. A. 2011;375:845–848.
[11] Gebhardt J, Koch RJ, Zhao W, et al. Growth and electronic structure of boron-doped graphene. Phys. Rev. B. 2013;87:155437.
[12] Kan EJ, Wu X, Li Z, et al. Half-metallicity in hybrid BCN nanoribbons. J. Chem. Phys. 2013;129:084712.
[13] Huzak M, Deleuze MS, Hajgató B. Half-metallicity and spin-contamination of the electronic ground state of graphene nanoribbons and related systems: An impossible compromise? J. Chem. Phys. 2011;135:104704.
[14] Grimme S, Antony J, Ehrlich S, et al. A consistent and accurate *ab initio* parametrization of density functional dispersion correction (DFT-D) for the 94 elements H-Pu. J. Chem. Phys. 2010;132:154104.
[15] TURBOMOLE V7.0. A development of University of Karlsruhe and Forschungszentrum Karlsruhe GmbH, 1989–2007, TURBOMOLE GmbH, since 2007. 2015. Available from: http://www.cosmologic.de/turbomole/home.html.
[16] Dunning TH Jr. Gaussian basis sets for use in correlated molecular calculations. I. The atoms boron through neon and hydrogen. Chem. Phys. 1989;90:1007–1023.
[17] Ditchfield R, Hehre WJ, Pople JA. Self-consistent molecular-orbital methods. IX. An extended Gaussian-type basis for molecular-orbital studies of organic molecules. J. Chem. Phys. 1971;54:724–728.
[18] Frisch MJ, Trucks GW, Schlegel HB, et al. Gaussian 09, Revision E.01, Wallingford, CT: Gaussian, Inc.; 2009.
[19] Hibino H, Kageshima H, Kotsugi M, et al. Dependence of electronic properties of epitaxial few-layer graphene on the number of layers investigated by photoelectron emission microscopy. Phys. Rev. B. 2009;79:125437.
[20] Rehaman A, Moughal S, Cramer CJ, et al. Second-order perturbation theory with complete and restricted active space reference functions applied to oligomeric unsaturated hydrocarbons. Phys. Chem. Chem. Phys. 2009;11:10964–10972.
[21] Castillo UJ, Guadarrama P, Fomine S. Large face to face tetraphenylporphyrin/fullerene nanoaggregates. A DFT study. Org. Electron. 2013;14:2617–2627.
[22] Hutchison GR, Ratner MA, Marks TJ. Hopping transport in conductive heterocyclic oligomers: reorganization energies and substituent effects. J. Am. Chem. Soc. 2005;127:2339–2350.
[23] Chen HC, Hsu CP, Reek JNH, et al. Highly soluble benzo[ghi] perylenetriimide derivatives: Stable and air-insensitive electron acceptors for artificial photosynthesis. Chem. Sus. Chem. 2015;8:3639–3650.
[24] Senevirathna W, Daddario CM, Sauvé G. Density functional theory study predicts low reorganization energies for azadipyrromethene-based metal complexes. J. Phys. Chem. Lett. 2014;5:935–941.
[25] Lin BC, Cheng CP, Lao ZPM. Reorganization energies in the transports of holes and electrons in organic amines in organic electroluminescence studied by density functional theory. J. Phys. Chem. A. 2003;107:5241–5251.
[26] Malagoli M, Brédas JL. Density functional theory study of the geometric structure and energetics of triphenylamine-based hole-transporting molecules. Chem. Phys. Lett. 2000;327:13–17.

[27] Sakanoue K, Motoda M, Sugimoto M, et al. A molecular orbital study on the hole transport property of organic amine compounds. J. Phys. Chem. A. 1999;103:5551–5556.
[28] Han MY, Brant JC, Kim P. Electron transport in disordered graphene nanoribbons. Phys. Rev. Lett. 2010;104:056801.
[29] Gruhn NE, da Silva Filho DA, Bill TG, et al. The vibrational reorganization energy in pentacene: molecular influences on charge transport. J. Am. Chem. Soc. 2002;124:7918–7919.
[30] Amashukeli X., Winkler J.R., Gray H.B., Gruhn N.E., Lichtenberger D.L. Electron-transfer reorganization energies of isolated organic molecules. J Phys Chem A. 2002;106:7593–7598.
[31] Darwent B. Bond dissociation energies in simple molecules, in: National Standarts Reference Data System, Washington, DC: National Bureau of Standards;1970. p. 31–52.